DR. HSING-JUH LIN (Orcid ID : 0000-0001-8322-7195)

Article type : Primary Research Articles

Title: Factors regulating carbon sinks in mangrove ecosystems

Running head: Carbon sinks in mangroves

List of authors: Shi-Bo Li[1], Po-Hung Chen[1], Jih-Sheng Huang[1], Mei-Li Hsueh[2], Li-Yung Hsieh[2], Chen-Lu Lee[3], Hsing-Juh Lin[1,3*]

Institute of origin:

[1]Department of Life Sciences and Innovation and Development Center of Sustainable Agriculture, National Chung Hsing University, Taichung 40227, Taiwan.

[2]Endemic Species Research Institute, Chichi 55244, Taiwan.

[3]Biodiversity Research Center, Academia Sinica, Taipei 11529, Taiwan.

***Corresponding author**: Hsing-Juh Lin (hjlin@dragon.nchu.edu.tw), +886-4-22840416#511

Keywords: *Avicennia marina*, Carbon budget, Carbon burial, Decomposition, *Kandelia obovata*, Net production

This article has been accepted for publication and undergone full peer review but has not been through the copyediting, typesetting, pagination and proofreading process, which may lead to differences between this version and the Version of Record. Please cite this article as doi: 10.1111/gcb.14322

Paper type: Primary Research Article

Abstract

Mangroves are recognized as one of the richest carbon storage systems. However, the factors regulating carbon sinks in mangrove ecosystems are still unclear, particularly in the subtropical mangroves. The biomass, production, litterfall, detrital export and decomposition of the dominant mangrove vegetation in subtropical (*Kandelia obovata*) and tropical (*Avicennia marina*) Taiwan were quantified from October 2011 to July 2014 to construct the carbon budgets. Despite the different tree species, a principal component analysis revealed the site or environmental conditions had a greater influence than the tree species on the carbon processes. For both species, the net production (NP) rates ranged from 10.86–27.64 Mg C ha^{-1} yr^{-1} and were higher than the global average rate due to the high tree density. While most of the litterfall remained on the ground, a high percentage (72–91%) of the ground litter decomposed within one year and fluxed out of the mangroves. However, human activities might cause a carbon flux into the mangroves and a lower NP rate. The rates of the organic carbon export and soil heterotrophic respiration were greater than the global mean values and those at other locations. Only a small percentage (3–12%) of the NP was stored in the sediment. The carbon burial rates were much lower than the global average rate due to their faster decomposition, indicating that decomposition played a critical role in determining the burial rate in the sediment. The summation of the organic and inorganic carbon fluxes and soil heterotrophic respiration well exceeded the amount of litter decomposition, indicating an additional source of organic carbon that was unaccounted for by decomposition in the sediment. Sediment-stable isotope analyses

further suggest that the trapping of organic matter from upstream rivers or adjacent waters contributed more to the mangrove carbon sinks than the actual production of the mangrove trees.

Introduction

Atmospheric CO_2 concentrations have been dramatically altered by human perturbations to the global carbon cycle. For the past 150 years, approximately 75% of the cumulative emissions of CO_2 have been derived from fossil fuels and industry, and 25% have been derived from land-use changes such as deforestation (Le Quéré *et al*., 2016). Mitigation strategies leading to significant reductions in atmospheric CO_2 concentrations might be an effective solution to prevent the mostly irreversible impacts of climate change on marine ecosystems and their services (Gattuso *et al*., 2015). Blue carbon refers to the preservation of carbon within marine ecosystems. Enhancing carbon storage by conserving or restoring coastal ecosystems can mitigate the global CO_2 imbalance and help reduce climate change (Nellemann *et al*., 2009). Compared to terrestrial ecosystems, the sediments of coastal ecosystems might accumulate more organic carbon due to their anoxic environments and the slow decomposition rate of organic matter (Duarte *et al*., 2011). The carbon sequestration in coastal ecosystems is 2–4 times that sequestered by tropical forests, and the carbon stock in coastal ecosystems is 3–5 times the amount stored in tropical forests (Donato *et al*., 2011). Coastal and estuarine ecosystems store 16.5 million tons of CO_2 each year, accounting for almost half of the global transportation emissions (Nellemann *et al*., 2009). Coastal ecosystems are considered to be the most efficient carbon sinks on Earth and play a critical role in regulating the regional and global carbon cycle.

Mangroves, the only woody plants that grow at low latitudes between the land and sea, cover 17 million hectares mostly in tropical regions (Lugo and Snedaker, 1974). Mangroves have been recognized as one of the richest carbon storage systems in tropical forests (Kauffman *et al*., 2011). The high productivity of mangroves is comparable to the productivity of tropical moist evergreen forests and coral reefs (Duarte *et al*., 2010; Donato *et al*., 2011; Alongi, 2014). Although mangroves only account for 0.7% of the area of tropical forests and 0.1% of the global land surface area (Giri *et al*., 2011), their net production (218 Pg yr^{-1}) accounts for half of the net production of the global coastal ecosystems (Bouillon *et al*., 2008). Mangroves have higher carbon stocks (up to 1,023 Mg ha^{-1}) than do salt marshes, seagrass beds, peatland and other major global forests (Adame *et al*., 2013; Alongi, 2014; Donato *et al*., 2011; Kelleway *et al*., 2016), as mangroves have woody biomass and a high root:shoot ratio and 88% of their organic carbon is stored in sediments deeper than 3 meters (Donato *et al*., 2011). Due to their high productivity, large amount of stored carbon, soil moisture characteristics and the deposition of organic matter from upstream rivers or adjacent coastal waters, mangroves are sites of high, effective carbon sinks (Wolanski, 1995; Atwood *et al*., 2017; Howard *et al*., 2017). However, the factors regulating carbon sinks in mangrove ecosystems are still unclear.

Twilley *et al*. (1992) first compiled the available data on the biomass, wood production, sedimentation, litterfall and export of mangroves to estimate a preliminary global carbon budget. They indicated that the river discharge of organic carbon and coastal eutrophication may alter the carbon cycle in mangrove ecosystems. Bouillon *et al*. (2008) synthesized data on carbon processes in mangrove ecosystems and found that >50% of the carbon fixed by mangrove vegetation was not adequately quantified. Christensen *et al*. (2008) reviewed the

production, composition, transport, pathways and transformation of organic carbon in mangrove ecosystems and found that most mangrove detritus that entered the sediment was degraded by microorganisms. They indicated that a complete understanding of the variability of carbon processes in different environmental conditions is lacking. Breithaupt *et al*. (2012) added more data from some of the largest, most developed mangrove forests in the world and found that the burial fraction was 42% larger than that of previous carbon budgets (Bouillon *et al*., 2008). Ray *et al.* (2013) constructed the carbon budget for the Indian Sundarbans mangroves and found only a small percentage (0.18%) of the net production was buried in the sediment. The carbon budget (Ray *et al*., 2013) showed a significant part (16%) of the net production was unresolved, which was referred to as 'missing carbon'. Ray *et al*. (2018) further reported that an export of mangrove-derived carbon exceeding the 'missing carbon' and indicated that the carbon budget had to be balanced by other unknown processes. Lee *et al.* (2014) reported that mangroves in different environments may produce and store carbon in different ways. They also indicated that little is known about dissolved carbon in mangrove carbon budgets. Together, these results indicate that more empirical work on carbon processes is needed to reduce uncertainties about the contribution of mangrove ecosystems to blue carbon, particularly in the subtropical mangroves, as they represent a classical and specific forest type that is very different from the tropical mangroves that have been extensively studied (Atwood *et al*., 2017; Lee *et al*., 2014).

In the past century, approximately 35% of the mangrove habitats have disappeared (Valiela *et al*., 2001), and the decline is continuing at a rate of 1–3% every year (Mcleod *et al*., 2011). Donato *et al*. (2012) indicated that mangrove deforestation generates as much as

approximately 10% of the emissions from global deforestation. Given the high potential impact of mangroves on the sedimentation of riverine suspended matter and the exchange of organic matter and nutrients in coastal waters, such high losses or the severe degradation of their functioning can coincide with significant changes in the coastal carbon cycle (Christensen *et al*., 2008). Using the dominant mangrove vegetation in tropical and subtropical Taiwan under different circumstances as examples, the objectives of this study were to 1) quantify the biomass, production, litterfall, detrital export and decomposition of the mangrove ecosystems, 2) determine whether there is vegetation variation in these processes, 3) examine whether there is spatial variation in these processes, 4) estimate the organic carbon burial rates by integrating the processes described above, and 5) trace the sources of organic carbon in the sediments of mangroves using stable isotope analyses.

Materials and methods

Study sites

Mangroves are widely distributed along the western coast of Taiwan and are subjected to a semidiurnal tidal regime. Northern Taiwan has rain year-round, while southern Taiwan is rainy in summer and dry in winter. While the species *Kandelia obovata* is dominant in northern (subtropical) Taiwan, *Avicennia marina* is the dominant species in southern (tropical) Taiwan. To collect representative samples across different geographic regions, mangroves at four natural sites in northern, central, and southern Taiwan were studied (Table 1). The first study site was located in the Danshuei River estuary (DK) in northern Taiwan. At the DK, the distribution area of *K. obovata* is 55 ha. The second and third sites were located in the *K. obovata* (EK) and *A. marina* (EA) mangrove forests, respectively, in the

Erhlin Stream estuary in central Taiwan. At these sites, the distribution area of *K. obovata* and *A. marina* is 4.9 ha and 17.1 ha, respectively. The fourth site was located in the Chiku Stream estuary (CA) in southern Taiwan. At the CA, the distribution area of *A. marina* is 4.7 ha. At each site, 3 quadrats (measuring 5 x 5 m) separated from each other by 15 m were randomly selected for sampling in the mangrove forest.

Conceptual carbon budget

The annual carbon budgets, in terms of g C m^{-2} yr^{-1}, of the mangroves at the four study sites were constructed by transforming data on the dry weight (DW) to carbon weight by multiplying the carbon content and integrating the seasonal data on the aboveground and belowground biomass, production and litterfall and the detrital export and decomposition. These processes followed the conceptual model shown in Fig. 1 (modified from Bouillon *et al*., 2008) and were quantified from October 2011 to January 2014.

Growth and litterfall

The net production (NP) of mangroves for each species was measured using the summation method (Kira and Shidei, 1967) shown in Eq. (1). We assumed that the grazing effect (ΔG) was low due to the low occurrence of herbivores directly feeding on mangrove tissues in Taiwan (Lin *et al*., 2007a). The amount of litterfall from the belowground structures was also relatively small (a small part of ΔL), so only the change in biomass (ΔB) and the amount of litterfall from the aboveground structures (a large part of ΔL) were determined in this study.

$$\mathrm{NP\ (g\ DW\ m^{-2}\ d^{-1})} = \Delta B + \Delta L + \Delta G \qquad (1)$$

The growth of mangroves (ΔB) was estimated by the increase in mangrove biomass per unit time. The allometric equations used to estimate the mangrove biomass in this study were first examined by constructing linear regressions of the estimated vs. the actual aboveground biomass. Mangrove allometry is site- and species-specific (Komiyama *et al*., 2008). Thus, samples of the aboveground structures from 9 stems of *A*. *marina* or *K*. *obovata* covering different size classes with varying diameters were harvested by covering the trees with nets to prevent losses of leaves, fruits and branches when handling. The height (H, m), the diameter at breast height (DBH, cm) and the diameter at 10% of the height above the ground ($D_{0.1}$, cm) of all the stems of *A*. *marina* and *K*. *obovata* were measured. All the leaves, branches, roots, fruits, flowers and stem pieces were sorted and weighed. These materials were weighed again after drying in an oven at 75°C for 7 days or until a constant weight was reached. The coefficients of determination (R^2) were 0.93–0.98, and the slopes were 0.71–1.09 for the aboveground biomasses of both species. These results indicate that the allometric equations given in Appendix S1 were appropriate for use in this study. Since it was difficult to harvest all belowground structures more than 50 cm below the surface, the belowground biomass was estimated using the allometric equations given in Appendix S1, which were proposed by other studies rather than based on our data.

All mangrove trees over 2.5 cm in DBH within the three quadrats at each site were measured every three months for a whole year to determine the H, DBH and $D_{0.1}$. These parameters were then used as the inputs for the derived allometric equations of *K. obovata* or *A. marina* (Appendix S1) to estimate the increase in mangrove biomass. The carbon content of the dried materials was also analyzed using an elemental analyzer (Elementar

Vario EL III CHNOS Rapid F002, Heraeus, Germany) after grounding the materials to a fine powder. The accuracy of the measurements was ± 0.1% and the precision was ± 0.2%.

During the study period, three litterfall collecting baskets (42 cm diameter, with a mesh size of 1 mm) were placed within each quadrat and retrieved every two months. The collected litterfall in the three baskets was pooled into one sample for each quadrat. After drying the litterfall in an oven at 75°C for at least 4 days, the production rate of the litterfall within each quadrat was determined as shown in Eq. (2).

$$LF = \frac{L1+L2+L3}{3\times a\times d} \quad (2)$$

where *LF*: production rate of litterfall per unit area in dry weight (g DW m^{-2} d^{-1}), *L1, L2, L3*: the amount of litterfall in dry weight in the three baskets (g DW), a: the area of the opening of the litterfall collecting basket (m^2), and d: the litterfall collection time in days.

The fate of litterfall (*LF*) can be further described as follows:

$$LF = DE + DD + DS, \quad (3)$$

where *DE* is the amount of detritus exported to nearshore waters by tides and waves, *DD* is the amount of detritus that decomposes, and *DS* is the amount of detritus stored in the soil in the form of refractory detritus within the year. *DD* was estimated by multiplying the decomposition rate (*K*) of detritus for the year described below by *LF*. *DS* was then estimated by subtracting *DE* and *DD* from *LF*.

Detrital export

To determine the export rate of leaves or detritus, three cubic-shaped grated stainless-steel net cages (30 cm x 30 cm opening, 60 cm length, and a mesh size of 1 mm, modified from Bach *et al*. (1986)) were placed randomly along the edge of each quadrat at each site in each season. Each net cage was surrounded with 5–10 floating balls and hung between two 2.5 m rods. The opening of the net cage faced the sea during flooding tides and faced the mangroves during ebbing tides. After a tidal cycle, all leaves or detritus leaving (positive direction) or entering (negative direction) the forest via tides, waves and floating on the surface were considered detrital export from or import to the mangroves, respectively. The leaves or detritus were collected from the net, rinsed quickly with fresh water, sorted, and dried at 60°C to a constant weight. The procedure was repeated for 3 days, with three replicates performed around the spring tide in each season for each quadrat. The export or import rates of detritus were expressed as the DW per unit area of mangroves per day (g DW m^{-2} d^{-1}).

Decomposition

To estimate the decomposition rate of detritus in the sediment, the freshly fallen leaves or branches of each mangrove species were collected from the mangroves at the four sites. The leaves or branches were rinsed quickly with fresh water and weighed in the laboratory, and the wet weights (WWs) were then transformed to DWs by multiplying by the WW-DW conversion factor. The leaves and branches (approximately 20 g WW each) were separated into different litterbags (10 x 10 cm, with a mesh size of 2 mm). Different species were also deposited into different litterbags. Three litterbags for each portion of each species at each

site on each visit were recovered. The litterbags of the leaves or branches were installed at the sediment surface at DK in November 2015 and recovered on days 7, 22, 57, 101, 149 and 219. The litterbags were installed at the sediment surface at EK and EA in May 2014 and recovered on days 7, 19, 35, 60, 80, 138 and 231. The litterbags were installed at the sediment surface at CA in December 2013 and recovered on days 7, 21, 56, 118 and 136. The recovered leaves or branches were again rinsed quickly with fresh water and dried at 60°C to a constant weight to determine the proportion of the remaining litter. The loss of the mass from the litterbags was used as a measure of the litter decomposition rate.

The decay curve for each portion of each mangrove species at each site was traced following the exponential model (Olson, 1963):

$$W_t = W_o e^{(-kt)}, \quad (4)$$

where W_t is the weight of the litter remaining from initial weight W_o after time t, and *K* is the decomposition rate (d^{-1}). The decomposition rate was calculated by fitting an exponential regression for each portion of each mangrove species at each site. The recovered leaves or branches were also analyzed to determine the carbon content of the DW using an elemental analyzer (Elementar Vario EL III CHNOS Rapid F002, Heraeus, Germany).

Organic and inorganic carbon flux

To estimate the flux of particulate and dissolved organic and inorganic carbon from or into the mangroves, the water outside and inside the mangroves was sampled following the methods of Dausse *et al*. (2012) to determine the concentration differences. If the concentrations inside the mangroves are higher than outside, the particulate and dissolved

organic and inorganic carbon were exported from the mangroves, and vice versa. The sampling started 1 hour before high tide at spring tide, and duplicate water samples were collected every 20-30 minutes with acid-washed 100 ml bottles at each quadrat (i.e., 2 samplings during flood tide and 2 samplings during ebb tide). The water depth and current velocity inside and outside the mangroves were recorded using a flow meter (FlowTracker Handheld-ADV, SonTek, USA). The water samples were preserved in a cooler and brought back to the laboratory for further analyses.

To measure the particulate organic carbon (POC), the water samples were filtered through a 0.7-μm filter (Whatman GF/F). The filter was acid-washed with 1N HCl, and the carbon content was determined using an elemental analyzer (Elementar Vario EL III CHNOS Rapid F002, Heraeus, Germany). The filtered water samples were analyzed for total carbon (TC) using the Shimadzu TOC-L (Shimadzu, Japan) and high-temperature combustion (680°C) to break down all carbon compounds into carbon dioxide (CO_2) and measure its concentration. The additional filtered water samples were acidified to remove inorganic carbon, and the samples were analyzed for dissolved organic carbon (DOC) using the Shimadzu TOC-L. The concentrations of dissolved inorganic carbon (DIC) were then determined by subtracting the concentrations of DOC from those of TC.

Soil heterotrophic respiration

We measured CO_2 fluxes at the air-sediment interface in each quadrat during emersion at low tide in each season using benthic chambers following Lee *et al*. (2011). Each chamber was 30 cm in diameter and had a semicircular upper transparent acrylic cover fitted onto a

stainless steel ring. The steel ring was pushed into the sediment to a depth of 10 cm to enclose a 0.071-m^2 surface area in the chamber; the volume of the trapped air was 10.6 L. Changes in the CO_2 mole fraction (ppm) of the air above the sediment were monitored using an infrared CO_2 gas analyzer (Li-820, LI-COR, Lincoln, NE, USA). The data were recorded on a data logger (Li-1400, LI-COR, Lincoln, NE, USA) using a 30-s logging frequency. The CO_2 fluxes were then calculated by regressing the CO_2 concentration (μmol CO_2 mol^{-1} air) against time (min). The data on the CO_2 fluxes were recorded as carbon units (mg C m^{-2} h^{-1}), under the assumption that at 25°C, 1 atm pressure, and a molar mass of 12 g C mol^{-1} CO_2, the molar volume was 24.5 L mol^{-1}. We also monitored air temperatures inside and outside the chamber using a WatchDog Model 250 Data Logger (Spectrum Technologies, Plainfield, IL, USA). At each quadrat for each measurement, the benthic metabolism (mg C m^{-2} h^{-1}) was determined from three simultaneous *in situ* measurements between 10:00 and 14:00. To estimate the heterotrophic soil respiration, measurements were taken in complete darkness (under 100% shading by interposing screens) and multiplied by a factor of 0.6 (Trumbore *et al*., 1999).

Soil stable isotope analysis

To trace the sources of the organic matter stored in the soil of the mangroves, the organic matter was isolated from duplicate samples collected from the surface and the top 5, 10, 20 and 30 cm of the soil of the mangroves at DK, EA and CA in July 2016. The preparation techniques used for the isotope ratio measurements followed Lin *et al*. (2007a). The $\delta^{13}C$ and $\delta^{15}N$ values of the samples were determined using a continuous-flow isotope ratio mass spectrometer (Finnigan delta S) coupled with an elemental analyzer (Carlo Erba NA 1500

NCS). The results for nitrogen and carbon isotopes are expressed in the usual delta notation relative to atmospheric nitrogen and Pee Dee Belemnite standards. The precision of the measurements was ± 0.1‰ for both the stable carbon and nitrogen isotope analyses.

Data analysis

One-way ANOVA was used to examine if the aboveground and belowground growth rates and the NP rate differed among the four study sites. Two-way ANOVA was used to examine if the detrital export rate and the soil heterotrophic respiration rate differed among seasons and sites. If significant differences were detected, Tukey's test was used to determine which means differed. Prior to the analysis, the data were examined to determine whether they conformed to the assumptions regarding normality and homogeneity of variance after the application of an appropriate transformation (Clarke and Warwick, 2001). These univariate statistical calculations were performed with SigmaPlot (version 12.5; Systat Software Inc., San Jose, CA, USA). A principal component analysis (PCA) was applied to reduce the complex data set of mangrove carbon processes to a low dimension to reveal hidden major factors influencing the carbon processes at the four mangrove forests. The PCA statistics were computed using PRIMER 6.1.13 and PERMANOVA+ (Clarke and Gorley, 2006).

Results

Structural characteristics

At DK, the mean density of *K. obovata* was 14033 trees ha^{-1} with a mean height of 3.8 m and a total biomass (aboveground and belowground) of 115.2 Mg DW ha^{-1} (Table 1). The mean water NH_4^+ concentration was 1–2 orders of magnitude higher than that at the other three

sites. The mean dissolved oxygen in the water reached almost zero in the summer. The mean density and total biomass of *K. obovata* were higher at EK. The tidal amplitude, reaching 3–4 m, was higher than that at the other sites. The mean water NO_x^- (NO_2^-+NO_3^-) concentration was 3–5 times lower than that at the other sites. At EA, the mean density of *A. marina* was 9900 trees ha^{-1} with a mean height of 1.8 m and a total biomass of 159.5 Mg DW ha^{-1}. Although the mean density of *A. marina* at CA was lower than that at EA, the mean height and total biomass were higher. The organic content in the sediment was also higher at CA, with a high variation.

Growth and litterfall

There were significant differences in the mangrove growth rates among the four study sites (Appendix S2). The aboveground growth rate was highest in *K. obovata* at EK (6.20 g DW m^{-2} d^{-1}) and lowest in *K. obovata* at DK (2.52 g DW m^{-2} d^{-1}) (Fig. 2a). The belowground growth rate was also highest in *K. obovata* at EK (3.71 g DW m^{-2} d^{-1}) and lowest in *K. obovata* at DK (1.07 g DW m^{-2} d^{-1}). The belowground growth rate was approximately half the aboveground growth rate. Consequently, the total growth rate, which was determined by summing the aboveground and belowground growth rates, was highest in *K. obovata* at EK (9.73 g DW m^{-2} d^{-1}) and lowest in *K. obovata* at DK (3.59 g DW m^{-2} d^{-1}).

The litterfall production rate corresponded well to the growth rate (Fig. 3). Leaves were the major components of the litterfall of the two species at the four study sites and contributed, in general, >50% of the composition (Appendix S3). The litterfall production of *K. obovata* was highest from April to August at both sites, as the percentages of propagules in

the total litterfall were the highest during this period. The higher production of litterfall occurred between September and October 2014 at EK and EA in the Erhlin Stream estuary due to the severe impacts of the Fungwong Typhoon on September 19, 2014. During this period, branches and leaves became the major components of the high production of litterfall. The mean litterfall production rate of *K. obovata* at DK and EK for a whole year was 9.75 Mg DW ha^{-1} yr^{-1} and 15.21 Mg DW ha^{-1} yr^{-1}, respectively. The litterfall production of *A. marina* was higher from April to October at both sites, which can be attributed to the production of propagules that reached up to 47% of the litterfall during this period. The mean litterfall production rate of *A. marina* at EA and CA for the whole year was 13.16 Mg DW ha^{-1} yr^{-1} and 12.46 Mg DW ha^{-1} yr^{-1}, respectively.

Consequently, the NP rates of the mangroves, which were determined by summing the aboveground and belowground growth and the litterfall production, were significantly higher for *K. obovata* at EK (10.36 g DW m^{-2} d^{-1}) than *K. obovata* at DK and *A. marina* at EA and CA (5.12-6.59 g DW m^{-2} d^{-1}) (Fig. 2b, Appendix S2).

Detrital export

There were no significant differences in detrital export rates among the four seasons for the two species at the four study sites due to their high variation (Appendix S2). For both species in the Erhlin Stream estuary (EK and EA), the rates of detrital export tended to be higher in the spring (Appendix S4). However, for *K. obovata* at DK and *A. marina* at CA, the rates of detrital export tended to be higher in the summer. The detrital export rate was lower in the winter for the two species at the four study sites.

The annual rates of detrital export from the mangroves were constructed by transforming data on DW to carbon weight by multiplying the averaged carbon content of each species at the different sites (i.e., DS: 48%, EK: 49%, EA: 46%, and CK: 45%), integrating the seasonal data on detrital export and weighting by the detrital composition of each structure at each site. Consequently, the annual rates of detrital export were estimated as 0.13 and 0.09 Mg C ha^{-1} yr^{-1} for *K. obovata* at DK and EK, respectively, and 0.15 and 0.68 Mg C ha^{-1} yr^{-1} for *A. marina* at EA and CA, respectively.

Decomposition

The leaf litter of the two species at the four sites decomposed rapidly within the first 20 days, and >50% of the DW had been lost after 50 days (Fig. 4a-d). Thereafter, the decomposition of the leaf litter slowed gradually, and only a small percentage of the DW remained in the litterbags after 136 days. The estimated decomposition rate of the leaves of *A. marina* at EA (0.0414 d^{-1}) was obviously faster than those of *A. marina* at CA and *K. obovata* at DK and EK (0.0148–0.0230 d^{-1}). The decomposition rate of the branch litter from *K. obovata* at DK (0.0005 d^{-1}) was 2 orders of magnitude slower than that of the leaf litter (Fig. 4e).

The amount of litterfall remaining on the sediment over a year was estimated by subtracting the amount of detrital export from the amount of litterfall. The annual rate of litter decomposition in the mangroves was then estimated by transforming the DW of the remaining litter to the carbon weight by multiplying the averaged carbon content and the decomposition rate of each species at the different sites for one year and weighting the rate by the percentages of leaves and branches in the litterfall for each species at each site. Consequently, the annual rates of litter decomposition were estimated as 3.21 and 6.73 Mg

C ha^{-1} yr^{-1} for *K. obovata* at DK and EK, respectively, and 5.98 and 4.05 Mg C ha^{-1} yr^{-1} for *A. marina* at EA and CA, respectively.

Organic and inorganic carbon flux

The fluxes of POC, DOC and DIC for the two species in the Erhlin Stream estuary (EK and EA) were apparently higher than those at the other two sites (Fig. 5). No significant difference in the fluxes was detected between the two species (Appendix S2). POC fluxed out of both species of mangroves at the four sites, particularly in the spring and summer. The highest flux of POC was observed from *A. marina* at EA in the spring, reaching 4.81 g C m^{-2} d^{-1}. Likewise, DOC also fluxed out of both species of mangroves at the four sites, and the higher outfluxes occurred mostly in the summer and winter. The highest flux of DOC was from *K. obovata* at EK in the winter, reaching 3.26 g C m^{-2} d^{-1}.

While DIC fluxed out of the *K. obovata* and *A. marina* mangroves, DIC fluxed into the *K. obovata* mangroves at DK during most of the time. For both species in the Erhlin Stream estuary (EK and EA), the fluxes of DIC were higher in the winter and spring. For *A. marina* at CA, however, the fluxes of DIC were higher in the summer. A higher DIC flux out of the *K. obovata* mangroves (7.68 g C m^{-2} d^{-1}) was observed at EK in the winter. A higher DIC flux out of the *A. marina* mangroves (8.50 g C m^{-2} d^{-1}) was also observed at EA in the spring.

Soil heterotrophic respiration

For the two species at the four sites, the soil heterotrophic respiration rate showed a significant interaction between the site and season (Appendix S2). The soil respiration rates

remained high in the *K. obovata* mangroves at DK from the spring to the fall (Appendix S5). For *K. obovata* at EK, however, the soil respiration rates were higher in every season except summer. For the *A. marina* growing at both sites (EA and CA), the soil respiration rates were high only in the summer.

Carbon budget

For *K. obovata* at DK, the NP was 10.86 Mg C ha^{-1} yr^{-1}, of which 86.83% was derived from aboveground growth and litterfall and 13.17% was derived from belowground growth (Fig. 6a). The aboveground growth and litterfall each accounted for approximately 50% of the NP. Most of the litterfall remained on the sediment and became ground litter. A small percentage of the litterfall (2.81% of the NP) fluxed out of the mangroves via tidal currents. A high percentage (71.5%) of the ground litter decomposed. Most of the decomposed litter fluxed out of the mangroves as POC (94.4%). Consequently, 1.27 Mg C ha^{-1} yr^{-1} or 11.69% of the NP was stored in the sediment. The stored NP was further respired by the benthic community via soil respiration (1.41 Mg C ha^{-1} yr^{-1}).

The NP of *K. obovata* at EK (27.64 Mg C ha^{-1} yr^{-1}) was much higher than that at DK. A total of 72.72% of the NP at EK was derived from aboveground growth and litterfall, and the other 27.28% was derived from belowground growth (Fig. 6b). The aboveground growth and litterfall accounted for 62.6% and 37.8% of the NP, respectively. Likewise, most of the litterfall remained on the sediment and became ground litter. Only a small percentage of the litterfall (0.33% of the NP) fluxed out of the mangroves via tidal currents. A very high percentage (88.9%) of the ground litter decomposed. Most of the decomposed litter fluxed

out of the mangroves as DOC (86.2%). Only 0.84 Mg C ha^{-1} yr^{-1} or 3.03% of the NP was stored in the sediment. The stored NP was further respired by the benthic community and fluxed out of the mangroves via DIC (16.2 Mg C ha^{-1} yr^{-1}).

The NP of *A. marina* at EA (15.37 Mg C ha^{-1} yr^{-1}) was lower than that of *K. obovata* in the same area, but a similar percentage (75.2%) was derived from the aboveground growth and litterfall, and the other 24.8% was derived from belowground growth (Fig. 6c). The aboveground growth and litterfall each accounted for approximately 50% of the NP. Likewise, most of the litterfall remained on the sediment and became ground litter. Only a small percentage of the litterfall (0.98% of the NP) flowed out of the mangroves via tidal currents. A very high percentage (91.1%) of the ground litter decomposed. The decomposed litter fluxed out of the mangroves as DOC (39.6%) and POC (66.6%). Likewise, only 0.57 Mg C ha^{-1} yr^{-1} or 3.70% of the NP was stored in the sediment. The stored NP was further respired by the benthic community and fluxed out of the mangroves via DIC (12.8 Mg C ha^{-1} yr^{-1}).

The NP of *A. marina* at CA was comparable to that of the same species at EA (12.64 Mg C ha^{-1} yr^{-1}), but a higher percentage (82.6%) was derived from the aboveground growth and litterfall, and the other 17.4% was derived from belowground growth (Fig. 6d). The aboveground growth and litterfall each accounted for approximately 50% of the NP. Likewise, most of the litterfall remained on the sediment and became ground litter. A higher percentage of the litterfall (5.37% of the NP) flowed out of the mangroves via tidal currents. Approximately 80% of the ground litter decomposed. Most of the decomposed litter fluxed out of the mangroves as POC (81.2%). Only 1.01 Mg C ha^{-1} yr^{-1} or 7.99% of the NP was stored in the sediment. Likewise, the stored NP was further respired by the benthic community and fluxed out of the mangroves as DIC (5.32 Mg C ha^{-1} yr^{-1}).

Soil stable isotopes

The mean $\delta^{13}C$ values of the organic matter collected from the soil of the mangroves ranged from -26.51‰ to -27.57‰ at the three study sites (Fig. 7). The mean $\delta^{13}C$ value of the soil organic matter was more enriched at a depth of 20–30 cm (> -27.25‰) than at the surface and at a depth of 10 cm (< -27.90‰) at CA (Appendix S2). Likewise, the mean $\delta^{13}C$ value of soil organic matter was more enriched at a depth of 10–30 cm (> -26.40‰) than at the surface and at a depth of 5 cm (< -26.97‰) at EA. However, there was no significant difference or a clear trend in the mean $\delta^{13}C$ values of the soil organic matter along the vertical profile at DK.

The mean $\delta^{15}N$ values of organic matter collected from the top 10 cm of the soil at CA (8.86‰–9.93‰) were significantly more enriched than those from the soil collected from > 20 cm deep (5.78‰ and 6.53‰) (Appendix S2). Likewise, the $\delta^{15}N$ values of organic matter collected from the soil surface at DK (4.70‰) were also significantly more enriched than were those from the 30-cm-deep soil (3.49‰). At EA, the mean $\delta^{15}N$ value of organic matter in the soil at 10-20 cm depths was apparently more enriched than the values collected from the surface and at 5 cm deep, but no significant difference was detected due to the high variation in the $\delta^{15}N$ values in the deeper soil (Fig. 7).

Discussion

Our results showed that the processes of the mangrove carbon budgets were more influenced by the site or environmental conditions than the mangrove tree species. Although *K. obovata* and *A. marina* were distributed in subtropical and tropical Taiwan, respectively, no significant differences in the aboveground growth, litterfall production and

NP rates were detected between the two species. However, there were significant spatial variations in most of the processes for each mangrove tree species. For both species, the aboveground growth, litterfall production, NP, decomposition rate and organic and inorganic carbon fluxes were higher in the Erhlin Stream estuary (EK and EA) than in the same species at the other site, which might be more related to the spatial variations in air temperature, humidity and fertility (*Keddy*, 2010). In contrast, the detrital export rates of both species were lower in the Erhlin Stream estuary (EK and EA) than in the same species at the other sites, which might also be related to the variations in tidal currents and geomorphology. The PCA analysis (Fig. 8) reveals that the seasonal carbon processes at EK and EA could be clearly separated from those at DK and CA by the first two PC axes (representing 65.8% of the variance). While the EK and EA mangroves were characterized by higher tree density and litterfall production and faster decomposition, the DK and CA mangroves generally had higher detrital export and soil heterotrophic respiration. Our findings echoed the argument of Kristensen *et al*. (2008) for the need to better understand the environmental factors responsible for the spatial variability in the carbon budget processes. To obtain a more accurate global carbon sink for mangrove ecosystems, reliable estimates of the carbon processes in mangrove vegetation across a broad geographic range and different environmental conditions are certainly needed (Atwood *et al*., 2017; Breithaupt *et al*., 2012; Lee *et al*., 2014).

The influence of human activities on carbon processes can be shown by the results at DK. Although the tree height and the aboveground biomass of *K. obovata* at DK were similar to those of *K. obovata* at Okinawa, the aboveground growth and NP rates were much lower than those of the same species or genus at other locations (Table 2). Chen (2014) reported

that *K*. *obovata* in the Danshui River estuary was threatened by the white-spotted longicorn beetle, *Anoplophora maculata*, which could lead to poor growth and the underestimation of the biomass. The Danshui River flows through the metropolitan area of Taipei City (> 6 million people) and receives large amounts of treated and untreated domestic sewage effluents. The river pollution index (RPI) from the 2016 annual report of the water quality of the Danshui River by the Environmental Protection Agency (http://wq.epa.gov.tw/Code/Report/ReportShow.aspx?ID=71&Languages=en) showed that more than 90% of the area of the estuary was moderately or heavily polluted. The vulnerable condition of the mangroves at DK is likely associated with the hypoxic conditions in the Danshui River (Lin *et al*., 2007b), which have resulted from the high loading rates of organic matter and dissolved inorganic nitrogen and phosphate (Wen *et al*., 2008) as a result of anthropogenic disturbances within the catchment. Consequently, the mean total biomass of the mangroves at DK (115.2 tons ha^{-1}, Table 1) was remarkably lower than the global mean (247 tons ha^{-1}) (Donato *et al*., 2012).

Moreover, contrary to the general pattern of DIC flux out of mangroves (Bouillon *et al*., 2008; Breithaupt *et al*., 2012), it was noted that there was a DIC flux into the mangroves at DK. Lin et al. (2007b) summarized the individual rate measurements of primary production and respiration in the Danshui River estuary and yielded an estimate of -95 g C m^{-2} yr^{-1}, which suggests a heterotrophic ecosystem and implies that more organic matter was consumed than was produced in the estuary. This difference might be the reason why the DIC concentration was higher in the river than in the mangroves. This finding also suggests that anthropogenic activity in the catchment might alter the carbon cycle of the downstream mangroves.

The higher levels of the aboveground growth and the litterfall production rate for *K. obovata* and *A. marina* growing at EK, EA and CA resulted in a greater aboveground NP rate. The aboveground NP rate for *K. obovata* at EK was much higher than that of the same species or genus at other locations (Table 2). The aboveground NP rates for *A. marina* at EA and CA were also higher than were those of the same species or genus at other locations. These values were approximately 2–3 times higher than the global average rate of wood production (12.08 Mg ha^{-1} yr^{-1}) (Twilley *et al*., 1992) and the global average rate of NP composed of litter and wood (13.63 Mg ha^{-1} yr^{-1}) (Bouillon *et al*., 2008). Consistent with the findings of Breithaupt *et al*. (2012), our results show the need to re-examine the underestimated global estimate of mangrove NP rate by taking into account data from the subtropical mangroves.

The high aboveground NP rate for *K. obovata* and *A. marina* growing at EK, EA and CA can be attributed to their high tree density. The mean tree heights of *K. obovata* at DK and Okinawa were comparable, but the mean density was higher at DK (Table 2). Consequently, the aboveground biomass and NP rate were much higher at EK than at DK and Okinawa. Similarly, the mean density of *A. marina* at CA was also higher than those at Dutch Bay and the scrub forest of Laguno de Terminos. The aboveground biomass and NP rate were thus much higher at CA. Interestingly, although the mean height was shorter at CA than the taller forest of Laguno de Terminos, the aboveground biomass and NP of *A*. *marina* at CA were still higher due to their higher density. The height of *A. marina* at EA was only 30% of that at the taller forest of Laguno de Terminos, but the density at EA was 6 times higher than that at the taller forest. Consequently, although the aboveground biomass was slightly lower, the aboveground NP was much higher at EA than at the taller forest. It appears that the main

factor affecting the aboveground NP rate is tree density. Ho et al. (2017) found the aboveground NP rate to increase with increasing tree density to a maximum point and then to decrease with increasing tree density for both *A*. *marina* and *K*. *obovata*, possibly due to the higher intraspecific competition. Their data suggested the maximum level of aboveground NP at a density of 30600 trees ha^{-1} for *K. obovata* and 10500 trees ha^{-1} for *A. marina*. This may explain the lower aboveground NP of *K. obovata* at Mai Po compared to EK, although the tree height and density were much higher at the former (Table 2).

Despite the higher NP of *K. obovata* at EK and *A. marina* at EA and CA than the same species or genus at other locations, their carbon storage or burial rates were much lower than the global mean values reported by Bouillon *et al*. (2008) and Breithaupt *et al*. (2012) (Table 3). Considering that the aboveground NP rates of these two species were comparable to those of other species in Southeast Asia (Table 2), it is likely that a high percentage of the NP was decomposed and that not much remaining NP was stored in the sediment. This difference is evident from the high decomposition rates of the two species at the four sites, which were remarkably faster than the global mean value (Bouillon *et al*., 2008) (Table 3). This finding suggests that decomposition plays a critical role in determining the burial of mangrove litter or blue carbon in the sediment, as indicated by Bouillon *et al*. (2008). However, this process has rarely been emphasized in previous field studies. The export of total organic carbon (TOC), which is composed of DOC and POC, in the four mangrove forests was also greater than the global mean value (Bouillon *et al*., 2008), although the areas of our studied mangroves were small (Table 3). Nevertheless, very limited data on the DOC and POC fluxes in mangroves are available for comparison. The soil heterotrophic respiration rates in the four mangrove forests were also higher than those estimated by the limited data

at other locations with comparable air temperatures (Table 4), as higher temperatures would increase heterotrophic respiration in the soil (Lee *et al*., 2011).

Maher *et al*. (2013) reported that DIC export averaged 3 g C m^{-2} d^{-1} and was an order of magnitude higher than DOC export in the mangroves. Their study considered DIC export to be similar to the global estimates of the missing carbon in mangroves (i.e., 1.9–2.7 g C m^{-2} d^{-1}). However, in this study, the mean values of TOC export ranged from 3.60–7.32 Mg C ha^{-1} yr^{-1} or 0.98–2.01 g C m^{-2} d^{-1} and were approximately 50%-75% of the global estimates of the missing carbon in mangroves. The mean DIC export rate was similar to the TOC export and ranged from 5.32–16.22 Mg C ha^{-1} yr^{-1} or 1.45–4.44 g C m^{-2} d^{-1}, with the exception of *K. obovata* at DK, where DIC fluxed into the mangroves from the heavily polluted river water as described above. The soil heterotrophic respiration rate ranged from 0.94–3.84 Mg C ha^{-1} yr^{-1} or 0.26–1.05 g C m^{-2} d^{-1} at the four sites and was approximately 20% of the DIC flux via tidal currents. Our results indicated that the global estimates of POC, DOC, DIC and soil heterotrophic respiration in the mangroves need more empirical data and should be revisited. With the exception of *K. obovata* at DK, the summation of the TOC, DIC and soil heterotrophic respiration well exceeds the amount of litter decomposition at the other three study sites. To balance the carbon budgets, the additional source of organic carbon unaccounted for in the decomposition in the sediments was likely derived from the detritus brought into the mangroves via floods caused by typhoons or heavy rainfall. These sources were not quantified in our carbon budgets and warrant further research to obtain a complete understanding of the underlying mechanisms leading to mangrove carbon sinks.

This deduction can be supported by the evidence of the soil stable isotope analyses in this study. In the Danshui Estuary, the mean $\delta^{13}C$ values of the dominant marsh plant *Phragmites communis*, the suspended particulate organic matter (SPOM), the benthic microalgae and *K. obovata* collected in the same season as ours (summer) were -26.9‰, -27.1‰, -24.1‰ and -28.2‰, respectively (Lin *et al.*, 2007a). The mean $\delta^{15}N$ values of the dominant marsh plant *Phragmites communis*, the SPOM, the benthic microalgae and *K. obovata* in the summer were 1.4‰, -2.4‰, 3.4‰ and 6.8‰, respectively (Lin *et al*., 2007a). In this study, the mean $\delta^{13}C$ and $\delta^{15}N$ values of the sediment in the top 30 cm of *K. obovata* soil at DS_K were -26.82‰ and 4.21‰, respectively, suggesting that marsh detritus contributed more to the accumulation of organic matter in the sediments than *K. obovata* itself. Likewise, in the Chiku Lagoon, the mean $\delta^{13}C$ values of the dominant C_3 marsh plants, SPOM, benthic microalgae and *A. marina* collected in the summer were -26.8‰, -23.5‰, -17.8‰ and -28.1‰, respectively (Lin *et al*., 2007b). The mean $\delta^{15}N$ values of the dominant C_3 marsh plants, SPOM, benthic microalgae and *A. marina* in the summer were 7.3‰, 7.1‰, 12.7‰ and 10.5‰, respectively (Lin *et al*., 2007a). The mean $\delta^{13}C$ and $\delta^{15}N$ values of the sediment in the top 30 cm of *A. marina* soils at CK were -27.5‰ and 8.05‰, respectively, indicating that the contribution of C_3 marsh plants to the organic matter of the sediment was more than the contribution of *A. marina*. Only a small fraction of mangrove production can be stored in the sediment. Our results suggest that the trapping of particulate organic matter from upstream rivers and adjacent coastal waters contributed more to the mangrove carbon sinks than the actual production of the mangrove trees, as indicated by Wolanski (1995). However, this process has been ignored and warrants further study in the future.

The main limitation of this study is the carbon processes of belowground NP. In this study, the allometric equations used to estimate the aboveground biomass were examined by constructing linear regressions of the estimated vs. the actual aboveground biomass. The coefficients of determination and the slopes indicated that the allometric equations for aboveground biomass were appropriate to use in this study. However, the allometric equations for belowground biomass could not be examined, as it was difficult to harvest all belowground structures more than 50 cm below the surface. This might be the case for *K. obovata*, as the belowground structures of an 8 cm DBH stand may reach >1 m deep (Cuc et al., 2009). Therefore, the belowground biomass was estimated using the allometric equations proposed by other studies rather than our data. This may underestimate the belowground NP. Belowground NP might contribute more to soil organic carbon than aboveground litterfall in mangroves due to the slower decomposition rate (Chen and Twilley, 1999; Middleton and McKee, 2001). Moreover, annual fine root production could be 1 to 3.5 times higher than litterfall production in mangroves (Xiong *et al*., 2017). As a matter of fact, little is known about herbivores directly feeding on mangrove belowground tissues. Therefore, the proportions of belowground NP that were consumed by animals, remained as detritus, were decomposed by microbes and finally were stored in the sediment were not considered. An additional source of organic carbon unaccounted for by the decomposition of litterfall in the sediments was possibly derived from the belowground detritus (Ouyang *et al*., 2017), though only a small fraction of mangrove production could be stored in the sediment.

Although *K. obovata* and *A. marina* were distributed in subtropical and tropical Taiwan, respectively, the carbon budgets showed a consistent pattern. For the two species, the NPs averaged 16.63 Mg C ha^{-1} yr^{-1}, of which more than 79% was derived from aboveground

growth and litterfall and 21% was derived from belowground growth. The aboveground growth and litterfall each accounted for approximately 50% of the aboveground NP. Most of the litterfall remained on the sediment and became ground litter. A small percentage of the litterfall (2.4% of the NP) flowed out of the mangroves via tidal currents. However, 83% of the ground litter decomposed in one year. Only 0.92 Mg C ha^{-1} yr^{-1} or 6.6% of the NP was stored in the sediment. The decomposed litter fluxed out of the mangroves as POC (66%) or DOC (48%). The summation of POC, DOC, DIC and soil heterotrophic respiration well exceeded the amount of litter decomposition, suggesting that the additional organic carbon that was unaccounted for by decomposition in the sediment was primarily derived from the trapped detritus from upstream rivers or adjacent marsh plants.

Acknowledgements

We are grateful for the support of the Ministry of Science and Technology of Taiwan under grant no. 103-2627-B-005-001 and 104-2621-M-005-002-MY2. This work was financially supported in part by the "Innovation and Development Center of Sustainable Agriculture" from The Featured Areas Research Center Program within the framework of the Higher Education Sprout Project by the Ministry of Education (MOE) in Taiwan. We kindly thank three anonymous reviewers for their constructive comments.

References

Adame MF, Lovelock CE (2011) Carbon and nutrient exchange of mangrove forests with the coastal ocean. *Hydrobiologia*, **663**, 23–50.

Adame MF, Kauffman JB, Medina I *et al.* (2013) Carbon stocks of tropical coastal wetlands

within the karstic landscape of the Mexican Caribbean. *PLoS One*, **8**, e56569.

Alongi DM, Tirendi F, Clough BF (2000) Below-ground decomposition of organic matter in forests of the mangroves *Rhizophora stylosa* and *Avicennia marina* along the arid coast of Western Australia. *Aquatic Botany*, **68**, 97–122.

Alongi DM, Wattayakorn G, Pfitzner J *et al*. (2001) Organic carbon accumulation and metabolic pathways in sediments of mangrove forests in southern Thailand. *Marine Geology*, **179**, 85–103.

Alongi DM (2014) Carbon cycling and storage in mangrove forests. *Annual Review of Marine Science*, **6**, 195–219.

Amarasinghe MD, Balasubramaniam S (1992) Net primary productivity of two mangrove forest stands on the northwestern coast of Sri Lanka. *Hydrobiologia*, **247**, 37–47.

Atwood TB, Connolly RM, Almahasheer H *et al.* (2017) Global patterns in mangrove soil carbon stocks and losses. *Nature Climate Change*, **7**, 523–528.

Bach SD, Thayer GW, Lacroix MW (1986) Export of detritus from eelgrass (*Zostera marina*) beds near Beaufort, north Carolina, USA. *Marine Ecology Progress Series*, **28**, 265–278.

Boto KG, Bunt JS (1981) Tidal export of particulate organic matter from a northern Australian mangrove system. *Estuarine, Coastal and Shelf Science*, **13**, 247–255.

Bouillon S, Borges AV, Castañeda- Moya E *et al.* (2008) Mangrove production and carbon sinks: a revision of global budget estimates. *Global Biogeochemical Cycles*, **22**, 1–12.

Breithaupt JL, Smoak JM, Smith TJ, Sanders CJ, Hoare A (2012) Organic carbon burial rates in mangrove sediments: strengthening the global budget. *Global Biogeochemical Cycles*, **26**, 1–11.

Bridgham SD, Patrick Megonigal J, Keller JK, Bliss NB, Trettin C (2006) The carbon balance of north American wetlands. *Wetlands*, **26**, 889–916.

Christensen B (1978) Biomass and primary production of *Rhizophora apiculata* BI. in a mangrove in southern Thailand. *Aquatic Botany*, **4**, 43–52.

Chen PH (2014) *Carbon stock and carbon budget of mangrove and marsh plants along the Danshui River* (master's dissertation), National Chung Hsing University, Taiwan.

Chen R, Twilley RR (1999) A simulation model of organic matter and nutrient accumulation in mangrove wetland soils. *Biogeochemistry*, **44**, 93–118.

Christensen SM, Tarp P, Hjortsø CN (2008) Mangrove forest management planning in coastal buffer and conservation zones, Vietnam: a multimethodological approach incorporating multiple stakeholders. *Ocean & Coastal Management*, **51**, 712–726.

Clarke KR, Gorley RN (2006) *PRIMER v6: user manual/tutorial*. PRIMER-E: Plymouth, United Kingdom.

Clarke KR, Warwick RM (2001) *Change in marine communities: an approach to statistical analysis and interpretation 2nd edition*. PRIMER-E: Plymouth, United Kingdom.

Cuc NTK, Ninomiya I, Long NT, Tri NH, Tuan MS, Hong PN (2009) Belowground carbon accumulation in young *Kandelia candel* (L.) Blanco plantations in Thai Binh River Mouth, Northern Vietnam. *International Journal of Ecology & Development*, **12**, 107–117.

Davis SE, Childers DL, Day JW, Rudnick DT, Sklar FH (2001) Wetland-water column exchanges of carbon, nitrogen, and phosphorus in a southern Everglades dwarf mangrove. *Estuaries*, **24**, 610–622.

Day Jr J, Coronado-Molina C, Vera-Herrera F, Twilley R, Rivera-Monroy V, Alvarez-Guillen H, Day R, and Conner W (1996) A 7 year record of above-ground net production in a southeastern Mexican mangrove forest. *Aquatic Botany*, **55,** 39–60.

Dausse A, Garbutt A, Norman L, Papadimitriou S, Jones LM, Robins PE, Thomas DN (2012) Biogeochemical functioning of grazed estuarine tidal marshes along a salinity gradient. *Estuarine, Coastal and Shelf Science*, **100**, 83–92.

Dittmar T, Lara RJ, Kattner G (2001) River or mangrove? Tracing major organic matter sources in tropical Brazilian coastal waters. *Marine Chemistry*, **73**, 253–271.

Dittmar T, Hertkorn N, Kattner G, Lara RJ (2006) Mangroves, a major source of dissolved organic carbon to the oceans. *Global Biogeochemical Cycles*, **20**, GB1012.

Donato D, Kauffman J, Mackenzie RA, Ainsworth A, Pfleeger A (2012) Whole-island carbon stocks in the tropical Pacific: implications for mangrove conservation and upland restoration. *Journal of Environmental Management*, **97**, 89–96.

Donato D, Kauffman JB, Murdiyarso D, Kurnianto S, Stidham M, Kanninen M (2011) Mangroves among the most carbon-rich forests in the tropics. *Nature Geoscience*, **4**, 293–297.

Duarte C, Agustí S (2011) Rapid carbon cycling in the oligotrophic ocean. *Biogeosciences Discussions*, **8**, 11661–11687.

Duarte CM, Marbà N, Gacia E, Fourqurean JW, Beggins J, Barrón C, Apostolaki ET (2010) Seagrass community metabolism: assessing the carbon sink capacity of seagrass meadows. *Global Biogeochemical Cycles*, **24**, 1–8.

Gattuso J-P, Magnan A, Billé R *et al.* (2015) Contrasting futures for ocean and society from

different anthropogenic CO_2 emissions scenarios. *Science*, **349**, aac4722.

Giri C, Ochieng E, Tieszen LL *et al.* (2011) Status and distribution of mangrove forests of the world using earth observation satellite data. *Global Ecology and Biogeography*, **20**, 154–159.

Gong WK, Ong JE (1990) Plant biomass and nutrient flux in a managed mangrove forest in Malaysia. *Estuarine, Coastal and Shelf Science*, **31**, 519–530.

Ho CW, Huang JS, Lin HJ (2017) Effects of tree thinning on carbon sequestration in mangroves. *Marine and Freshwater Research*, **69**, 1–10.

Howard J, Sutton-Grier A, Herr D *et al*. (2017) Clarifying the role of coastal and marine systems in climate mitigation. *Frontiers in Ecology and the Environment*, **15**, 42–50.

Jennerjahn TC, Ittekkot V (2002) Relevance of mangroves for the production and deposition of organic matter along tropical continental margins. *Naturwissenschaften*, **89**, 23–30.

Kauffman JB, Heider C, Cole TG, Dwire KA, Donato DC (2011) Ecosystem carbon stocks of Micronesian mangrove forests. *Wetlands*, **31**, 343–352.

Keddy PA (2010) *Wetland ecology: principles and conservation*. Cambridge University Press, Cambridge.

Kelleway JJ, Saintian N, Macreadie PI, Skibeck CG, Zawadzki A, Ralph PJ (2016) Seventy years of continuous encroachment substantially increase "blue carbon" capacity as mangrove replace intertidal salt marshes. *Global Change Biology*, **22**, 1097–1109.

Khan MNI, Suwa R, Hagihara A (2009) Biomass and aboveground net production in a subtropical mangrove stand of *Kandelia obovata* (S., L.) Yong at Manko Wetland, Okinawa, Japan. *Wetlands Ecology and Management*, **17,** 585–599.

Kira T, Shidei T (1967) Primary production and turnover of organic matter in different forest ecosystems of the western Pacific. *Japanese Journal of Ecology*, **17**, 70–87.

Komiyama A, Ong JE, Poungparn S (2008) Allometry, biomass, and productivity of mangrove forests: a review. *Aquatic Botany*, **89**, 128–137.

Kristensen E, Bouillon S, Dittmar T, Marchand C (2008) Organic carbon dynamics in mangrove ecosystems: a review. *Aquatic Botany*, **89**, 201–219.

Le Quéré C, Andrew RM, Canadell JG *et al.* (2016) Global carbon budget 2016. *Earth System Science Data*, **8**, 605–649.

Lee LH, Hsieh LY, Lin HJ (2011) *In situ* production and respiration of the benthic community during emersion on subtropical intertidal sandflats. *Marine Ecology Progress Series*, **441**, 33–47.

Lee SY (1990) Primary productivity and particulate organic matter flow in an estuarine mangrove-wetland in Hong Kong. *Marine Biology*, **106**, 453–463.

Lee SY, Primavera JH, Dahdouh-Guebas F *et al* (2014) Ecological role and services of tropical mangrove ecosystems: a reassessment. *Global Ecology and Biogeography*, **23**, 726–743.

Lin HJ, Kao WY, Wang YT (2007a) Analyses of stomach contents and stable isotopes reveal food sources of estuarine detritivorous fish in tropical/subtropical Taiwan. *Estuarine, Coastal and Shelf Science*, **73**, 527–537.

Lin HJ, Shao KT, Jan RQ, Hsieh HL, Chen CP, Hsieh LY, Hsiao YT (2007b) A trophic model for the Danshuei River Estuary, a hypoxic estuary in northern Taiwan. *Marine pollution bulletin*, **54**, 1789–1800.

Lovelock CE (2008) Soil respiration and belowground carbon allocation in mangrove forests. *Ecosystems*, **11**, 342–354.

Lugo AE, Snedaker SC (1974) The ecology of mangroves. *Annual Review of Ecology and Systematics*, **5**, 39–64.

Maher DT, Santos IR, Golsby-Smith L, Gleeson J, Eyre BD (2013) Groundwater- derived dissolved inorganic and organic carbon exports from a mangrove tidal creek: the missing mangrove carbon sink? *Limnology and Oceanography*, **58**, 475–488.

Machiwa JF (1999) Lateral fluxes of organic carbon in a mangrove forest partly contaminated with sewage wastes. *Mangroves and Salt Marshes*, **3**, 95–104.

Mcleod E, Chmura GL, Bouillon S *et al.* (2011) A blueprint for blue carbon: toward an improved understanding of the role of vegetated coastal habitats in sequestering CO_2. *Frontiers in Ecology and the Environment*, **9**, 552–560.

Middleton BA, McKee KL. (2001) Degradation of mangrove tissues and implications for peat formation in Belizean island forests. *Journal of Ecology*, **89**, 818–828.

Nellemann C, Corcoran E, Duarte CM, Valdes L, De young C, Fonseca L, Grimsditch G (2009) *Blue carbon. a rapid response assessment.* United Nations Environment Programme, GRID-Arendal.

Olson JS (1963) Energy storage and the balance of producers and decomposers in ecological systems. *Ecology*, **44**, 322–331.

Ouyang X, Lee SY, Connolly RM (2017) The role of root decomposition in global mangrove and saltmarsh carbon budgets. *Earth-Science Reviews*, **166**, 53–63.

Poungparn S, Komiyama A, Tanaka A *et al*. (2009) Carbon dioxide emission through soil

respiration in a secondary mangrove forest of eastern Thailand. *Journal of Tropical Ecology*, **25**, 393–400.

Putz FE, Chan HT (1986) Tree growth, dynamics, and productivity in a mature mangrove forest in Malaysia. *Forest Ecology and Management*, **17**, 211–230.

Ray R, Bauma A, Rixena T, Gleixner G, Jana TK (2018) Exportation of dissolved (inorganic and organic) and particulate carbon from mangroves and its implication to the carbon budget in the Indian Sundarbans. *Science of the Total Environment*, **621**, 535–547.

Ray R, Chowdhury C, Majumdar N, Dutta MK, Mukhopadhyay SK, Jana TK (2013) Improved model calculation of atmospheric CO_2 increment in affecting carbon stock of tropical mangrove forest. *Tellus* B, **65**, 18981.

Robertson AI (1986) Leaf-burying crabs: Their influence on energy flow and export from mixed mangrove forests Rhizophora in northeastern Australia. *Journal of Experimental Marine Biology and Ecology*, **102**, 237–248.

Romigh MM, Davis SE, Rivera-Monroy VH, Twilley RR (2006) Flux of organic carbon in a riverine mangrove wetland in the Florida Coastal Everglades. *Hydrobiologia*, **569**, 505–516.

Sukardjo S, Yamada I (1992) Biomass and productivity of a *Rhizophora mucronata* Lamarck plantation in Tritih, Central Java, Indonesia. *Forest Ecology and Management*, **49**, 195–209.

Trumbore SE, Bubier JL, Harden JW, Crill PM (1999) Carbon cycling in boreal wetlands: a comparison of three approaches. *Journal of Geophysical Research: Atmospheres*, **104**, 27673–27682.

Twilley RR (1985) The exchange of organic carbon in basin mangrove forests in a southwest Florida estuary. *Estuarine, Coastal and Shelf Science*, **20**, 543–557.

Twilley RR, Chen R, Hargis T (1992) Carbon sinks in mangroves and their implications to carbon budget of tropical coastal ecosystems. *Water, Air, & Soil Pollution*, **64**, 265–288.

Valiela I, Bowen JL, York JK (2001) Mangrove forests: one of the world's threatened major tropical environments. *Bioscience*, **51**, 807–815.

Wen LS, Jiann KT, Liu KK (2008) Seasonal variation and flux of dissolved nutrients in the Danshuei Estuary, Taiwan: a hypoxic subtropical mountain river. Estuarine, *Coastal and Shelf Science*, **78**, 694–704.

Wolanski E (1995) Transport of sediment in mangrove swamps. *Hydrobiologia*, **295**, 31–42.

Xiong Y, Liu X, Guan W, Liao B, Chen Y, Li M, Zhong C (2017) Fine root functional group based estimates of fine root production and turnover rate in natural mangrove forests. *Plant Soil*, **413**, 83–95.

Table 1. Structural and physicochemical parameters of the four studied mangrove forests along western Taiwan.

Site	DK	EK, EA	CA
Location	25°8’7"N, 121°27’32"E	23°56’3"N, 120°18’51"E	23°7’7"N, 120°5’20"E
Mangrove species	*Kandelia obovata*	*Kandelia obovata, Avicennia marina*	*Avicennia marina*
Area (ha)	55.0	4.9, 17.1	4.7
Mean tree height (m)	3.8	4.3, 1.8	4.0
Mean tree density (trees ha^{-1})	14033	21900, 9900	3200
Mean mangrove total biomass (Mg DW ha^{-1})	115.2	252.1, 159.5	188.5
Tidal amplitude (m)	1–2	3–4	1–2
Mean sediment organic carbon content in the top 30 cm (%)	1.38–2.50	0.51–0.65	0.67–11.01
Mean water temperature at high tide (°C)	15.4–30.7	17.2–29.9	15.8–31.6
Mean water salinity at high tide	3.4–25.7	18.7–35.0	13.9–32.9
Mean water dissolved oxygen at high tide (mg L^{-1})	0.4–11	3.9–6.5	4.3–9.3
Mean water NO_x^- concentration at high tide (µM)	11–37	4.6–13	23–57
Mean water NH_4^+ concentration at high tide (µM)	35–544	4.1–18	4.1–20
Mean water PO_4^{-3} concentration at high tide (µM)	1.0–11	1.6–9.4	2.8–5.9

Table 2. Comparison of structural characteristics and carbon processes in the mangrove forests of *Kandelia*, *Avicennia* and *Rhizophora* in Southeast Asia.

Species	Location (latitude)	H	D	AB	AG	LF	ANP	Reference
Kandelia obovata	Okinawa, Japan (26°N)	3.6	15475	80.5	21.5	10.6	32.1	Khan *et al*. (2009)
Kandelia obovata	DK (25°N)	3.8	14033	81.7	9.66	9.97	19.6	this study
Kandelia obovata	EK (24°N)	4.3	21900	152.4	25.7	15.6	41.0	this study
Avicennia marina	EA (24°N)	1.8	9900	61.4	12.0	14.6	25.1	this study
Avicennia marina	CA (23°N)	4.0	3200	104.3	10.5	12.7	23.2	this study
Kandelia candel	Mai Po, Hong Kong (22°N)	7	51770	129.6		11.1	24.4	Lee (1990)
Avicennia germinans (the scrub forest)	Laguno de Terminos, Mexico (18°N)	3-4	1720	17.4	0.62	3.07	3.99	Day *et al*. (1996)
Avicennia germinans (the taller forest)	Laguno de Terminos, Mexico (18°N)	6-7	1590	73.0	1.36	4.10	6.12	Day *et al*. (1996)
Avicennia marina	Dutch Bay, Sri Lanka (8°N)	3.5	3175		1.40	3.74	5.14	Amarasinghe and Balasubramaniam (1992)
Rhizophora apiculata	Phuket, Thailand	5-11		159	20	7.04	27	Christensen (1978)

	(7°N)							
Rhizophora mucronata	Tritih, Indonesia (7°N)	4-7	3300	93.7	14.6	10.4	25	Sukardjo and Yamada (1992)
Rhizophora apiculata	Matang, Malaysia (4°N)			409	6.7		17.7	Putz and Chan (1986)

H: tree height (m), D: tree density (trees ha^{-1}), AB: aboveground biomass (Mg DW ha^{-1}), AG: aboveground growth (Mg DW ha^{-1} yr^{-1}),

LF: litterfall (Mg DW ha^{-1} yr^{-1}), ANP: aboveground net production (Mg DW ha^{-1} yr^{-1})

Table 3. Comparison of area, carbon processes and export of particulate and dissolved organic carbon in the mangrove forests of this study and other studies.

Location	Area	ANP	LF	Decomp	Burial	POC	DOC	TOC	Reference
Global		13.63±4.5		2.63±1.93	1.15	1.37±1.72	1.50±1.34	2.52±2.77	Bouillon *et al*. (2008)
Global					1.63				Breithaupt *et al*. (2012)
Global	20,000,000		4.6					2.3	Jennerjahn and Ittekkot (2002)
DK	54	9.43	4.79	3.21	1.27	3.03	0.57	3.60	this study
EK	4.9	20.1	7.66	6.73	0.84	1.52	5.80	7.32	this study
EA	12.1	11.6	6.71	5.98	0.57	3.98	2.37	6.35	this study
CA	4.7	10.4	5.73	4.05	1.01	3.29	1.88	5.85	this study
Matang, Malaysia	40,800		3.51					1.76	Gong and Ong (1990)
Zanzibar, Tanzania						0.65	2.30	2.95	Machiwa (1999)
Florida, USA								6.57	Adame and Lovelock (2011)
Florida, USA							3.81		Davis *et al*. (2001)
Florida, USA			4.43					1.86	Twilley (1985)
Florida, USA						0.16	0.56		Romigh *et al*. (2006)

Amazon, Brazil	2,200			1.93	Dittmar *et al*. (2001)
Amazon, Brazil			1.44		Dittmar *et al*. (2006)
Chunda Bay, Australia		3.4			Robertson (1986)
Missionary Bay, Australia	500	4.2			Boto and Bunt (1981)
Moreton Bay, Australia			1.09		Maher *et al.* (2013)
Sundarbans, India	426,400	1.36	7.10	8.46	Ray *et al.* (2018)

Area (ha), ANP: above net production (Mg C ha^{-1} yr^{-1}), LF: litterfall (Mg C ha^{-1} yr^{-1}), Decomp: decomposition (Mg C ha^{-1} yr^{-1}), Burial (Mg C ha^{-1} yr^{-1}), POC: particulate organic carbon (Mg C ha^{-1} yr^{-1}), DOC: dissolved organic carbon (Mg C ha^{-1} yr^{-1}), TOC: total organic carbon (Mg C ha^{-1} yr^{-1})

Table 4. Comparison of soil heterotrophic respiration rates in the mangrove forests of this study and other studies.

Location	Soil heterotrophic respiration rate ($Mg\ C\ ha^{-1}\ yr^{-1}$)	Temperature (°C)	Reference
DK	1.41	15.4–30.7	this study
EK	3.84	17.0–29.9	this study
EA	0.94	17.0 –29.9	this study
CA	0.96	15.8–31.6	this study
Eastern Thailand	0.47	27.7–30.1	Poungparn *et al*. (2009)
Australia	0.05		Alongi *et al*. (2000)
Southern Thailand	0.20		Alongi *et al*. (2001)
Australia and New Zealand	0.38	15 – 35	Lovelock (2008)

Figure captions

Fig. 1. The conceptual carbon budget of the studied mangroves along western Taiwan. NP: net production; ANP: aboveground net production; BNP: belowground net production; DOC: dissolved organic carbon; POC: particulate organic carbon; DIC: dissolved inorganic carbon.

Fig. 2. Aboveground and belowground growth rates (a) and net production rates (b) in the four mangrove forests during the study period (mean±SE, n = 3).

Fig. 3. Litterfall production rates in the four mangrove forests during the study period (mean±SE, n = 3).

Fig. 4. Decomposition curves of leaves and branches (DK only) in the four mangrove forests during the study period (mean±SE, n = 3).

Fig. 5. Fluxes of particulate and dissolved organic and inorganic carbon in the four mangrove forests during the study period (mean±SE, n = 24).

Fig. 6. Annual carbon budgets of the four mangrove forests along western Taiwan.

Fig. 7. δ^{15}N vs. δ^{13}C of organic matter collected from the soil of three mangrove forests in July 2016 (mean±SD, n = 2).

Fig. 8. A principal component analysis (PCA) was conducted to reduce the data set of mangrove carbon processes to a low dimension to reveal hidden major factors influencing the carbon processes of the four mangroves along western Taiwan.

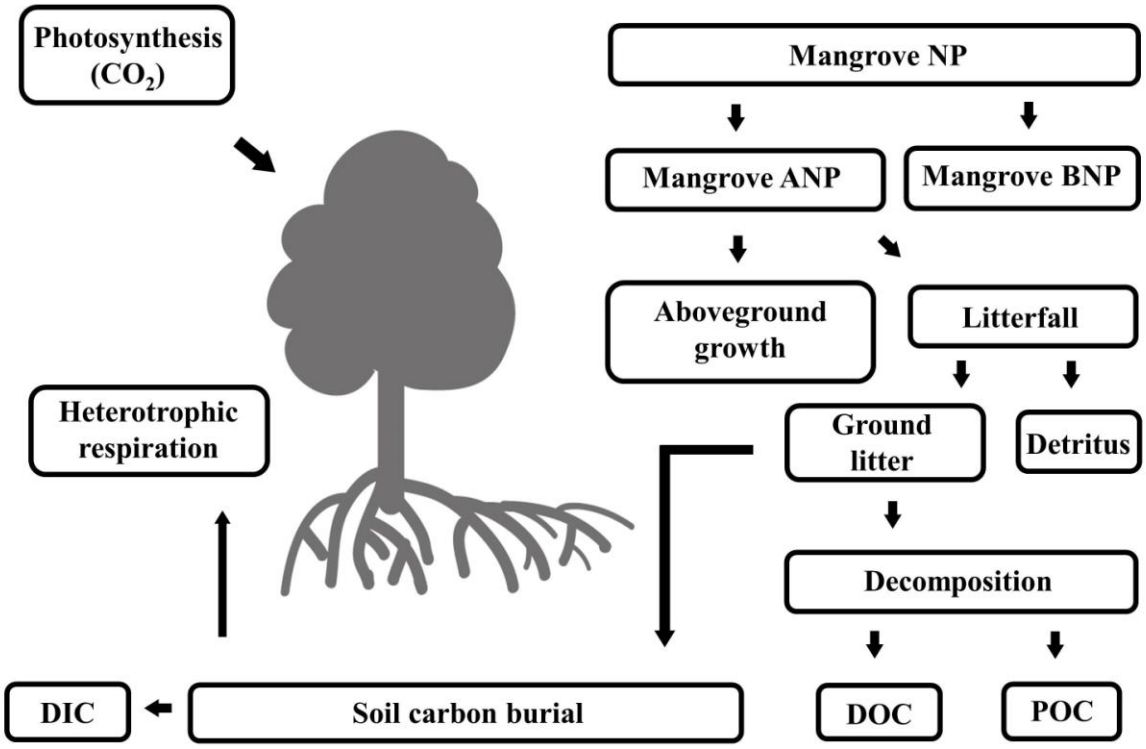

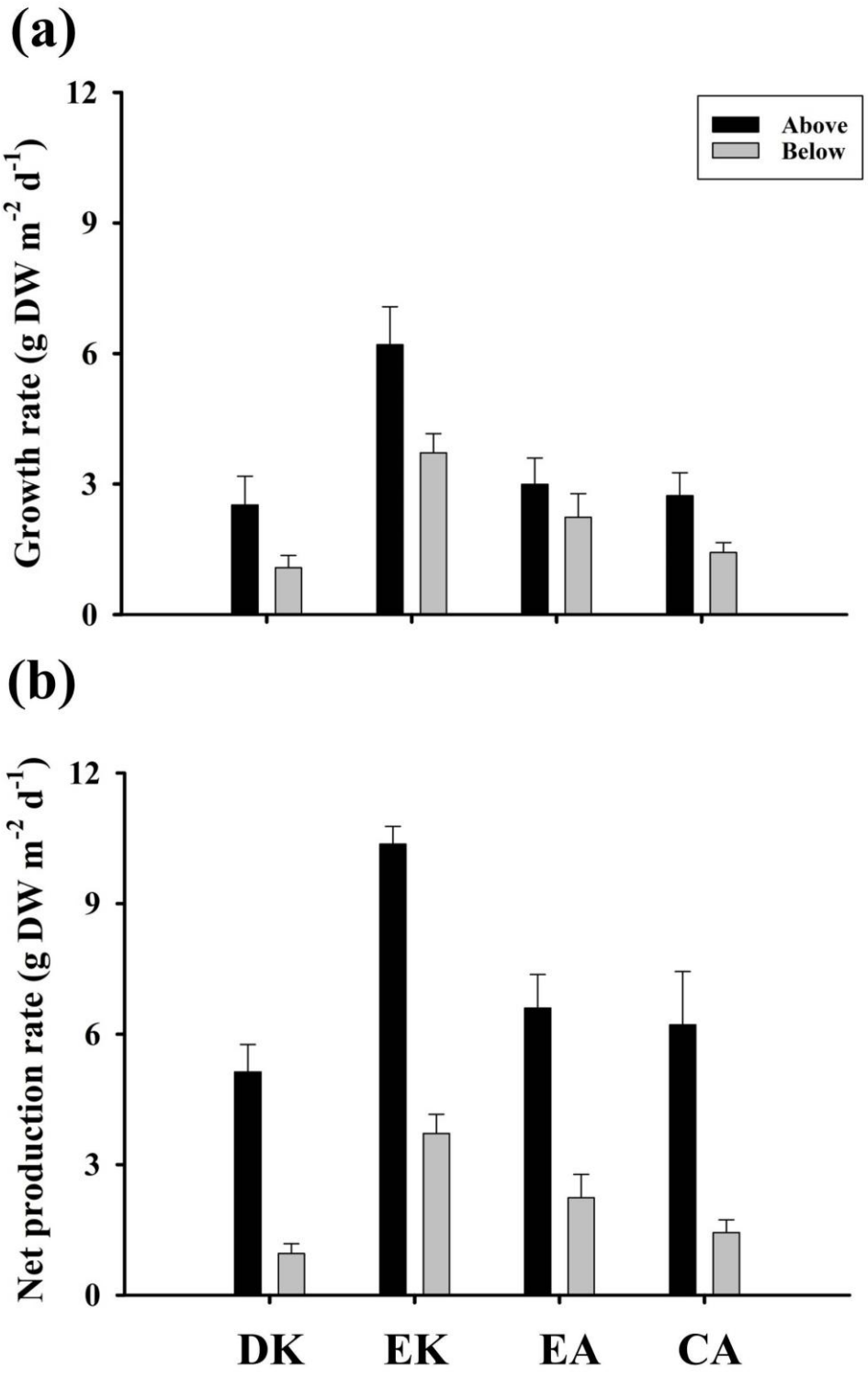

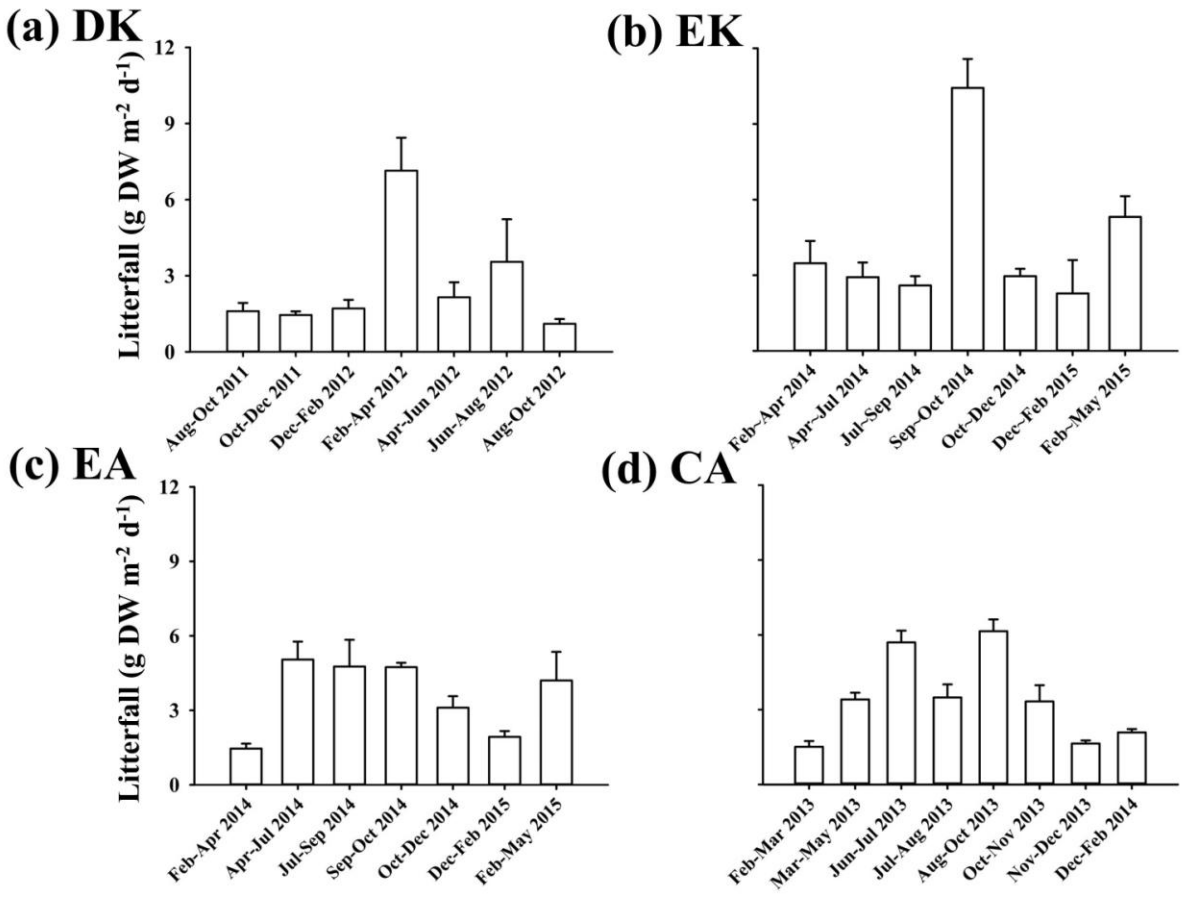

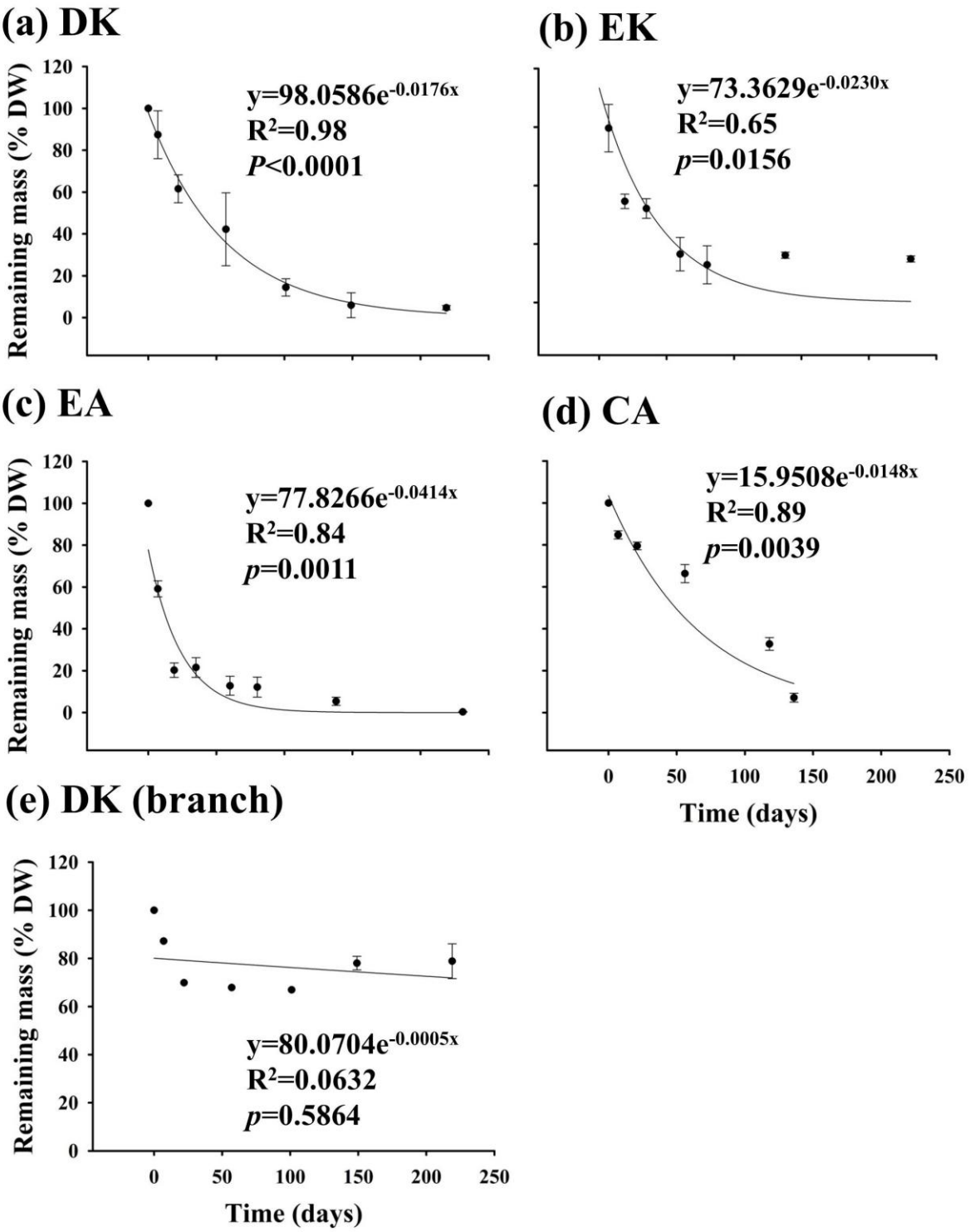

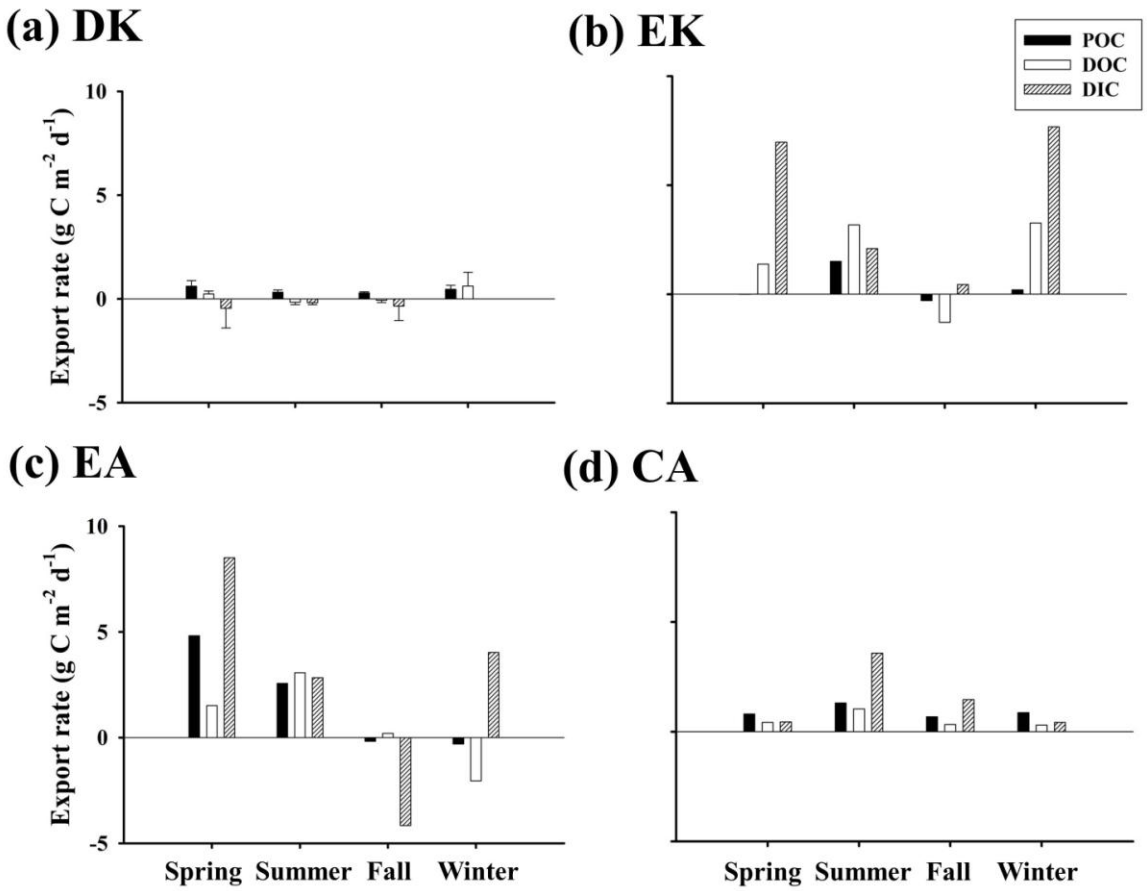

(a) DK

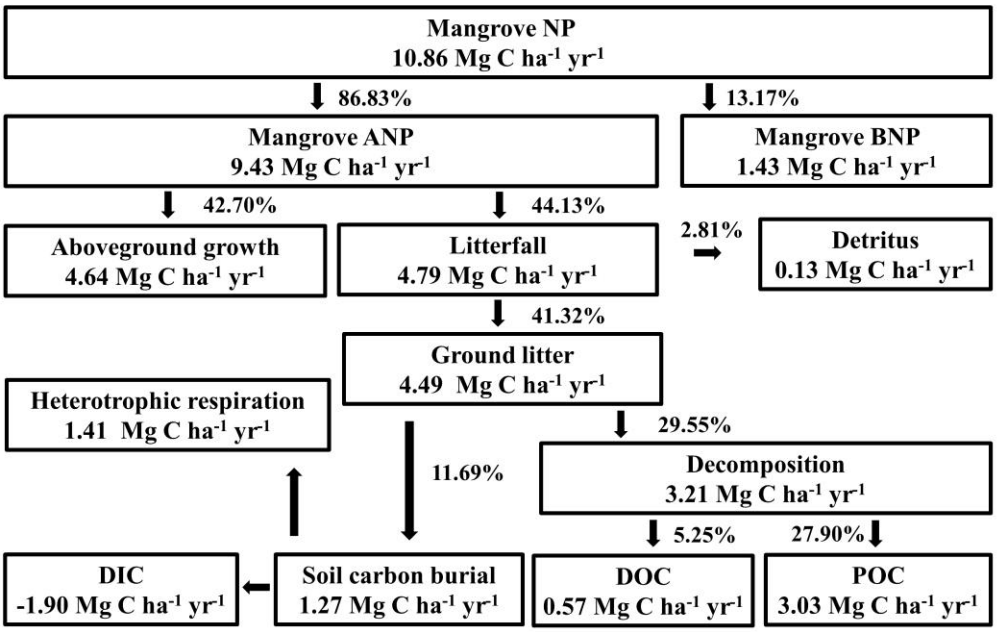

(b) EK

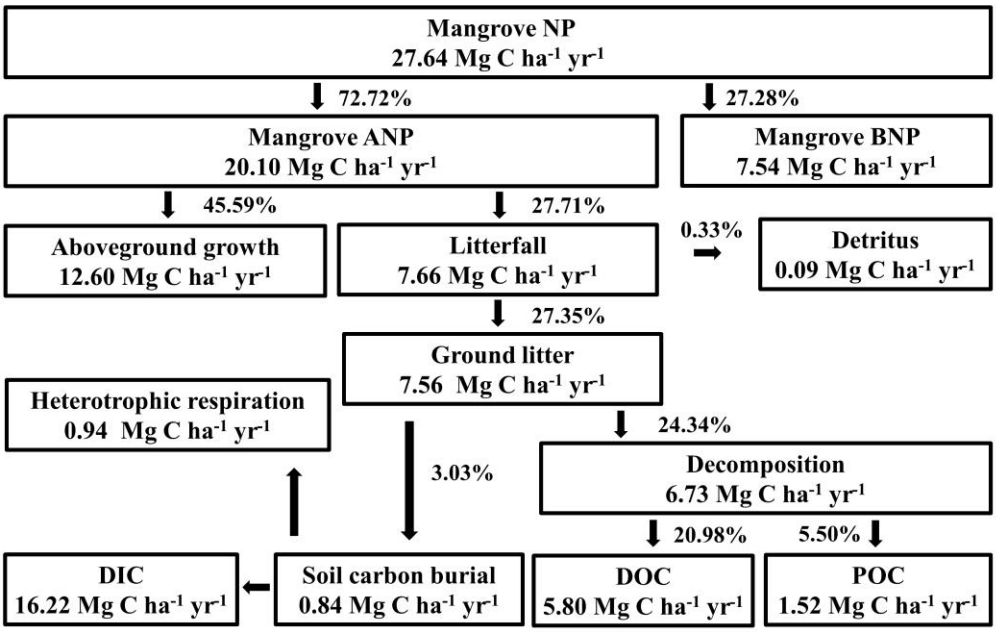

(c) EA

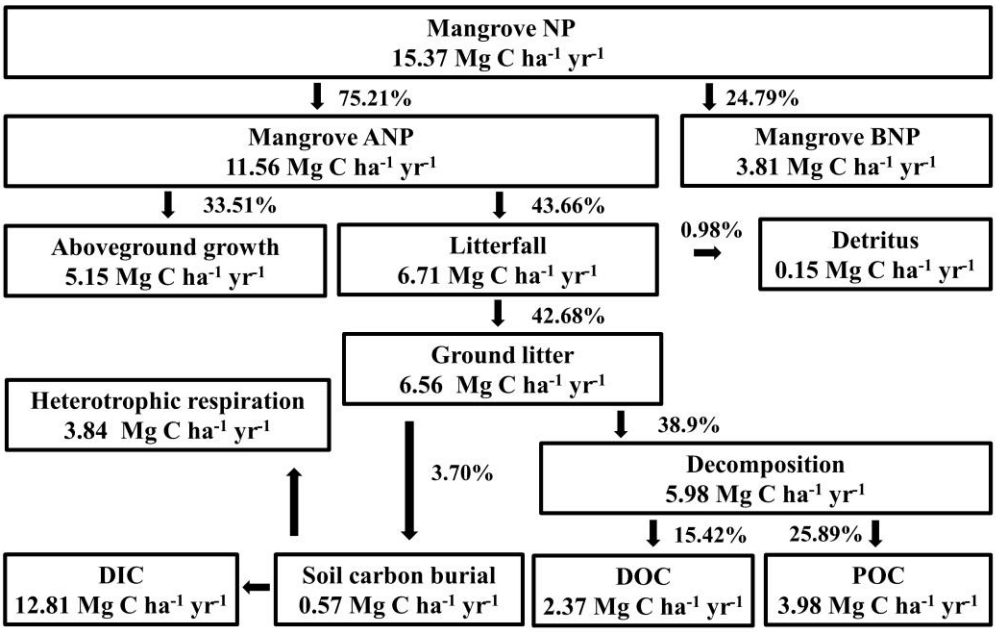

(d) CA